Variability-aware MMIC design through multiphysics modelling

Variability-aware MMIC design through multiphysics modelling

S. Donati Guerrieri, C. Ramella, E. Catoggio, F. Bonani
Dipartimento di Elettronica e Telecomunicazioni, Politecnico di Torino
Corso Duca degli Abruzzi, 24, I-10129 Torino, ITALY

***Abstract*—We present a novel multiphysics approach to the variability-aware modelling of MMIC stages, including technological variations in both the active devices and in the passive structures used to implement the matching networks. The models are based on accurate physical simulations via the TCAD numerical analysis of the active device, and electromagnetic simulations of the passives. Black-box models are then extracted and implemented into circuit simulators, using parameter-dependent X-parameters and scattering matrix. In both cases, the link with the underlying technology is always retained. After model validation, we present the statistical analysis of an X-band GaAs power amplifier. We show that the stage is highly affected by process induced variability, with spreads up to 3 dB of output power, 1.5 dB of operative gain, and more than 10 percentage points of drain efficiency.**

***Index Terms*—Multiphysics, Process Induced Variations; TCAD nonlinear Variability; physics-based co-simulation; EM simulations, Black-box models, MMIC circuits.**

I. Introduction

As the distinctive features of active device progress in terms of both electrical parameters (operating frequency, bandwidth, power handling capability etc.) and technology (semiconductor, gate length etc.) for microwave and mm-wave analog applications in advanced (and future) communication standards, a new challenge is found for the designer to cope with: the issue of Process Induced Variability (PIV) [1]–[5]. Furthermore, passive MMIC component PIV also plays a major role in determining the circuit robustness and yield [6]. As a consequence, efficient PIV-aware models for both the active device and the passive components are required to ascertain and, possibly, minimize variability effects on the design. The key requirement for a design-enabling model is its numerical efficiency, thus restricting the possible choices to compact models, either black-box or equivalent circuit-based, in conjunction with the capability to retain a link to technology, in order to allow for the description of perturbations vs. nominal parameter values.

In this contribution, we present an innovative variability-aware active and passive device modeling strategy, based on a multiphysics description of the electrical features as a function of technological parameters based on physics-based simulations: technology CAD (TCAD) for semiconductor devices, and an electro-magnetic (EM) description for passives. This modeling strategy is briefly introduced in Section II, and applied to the PIV analysis of a 12 GHz class-AB power amplifier (PA) in MMIC GaAs technology in Section III.

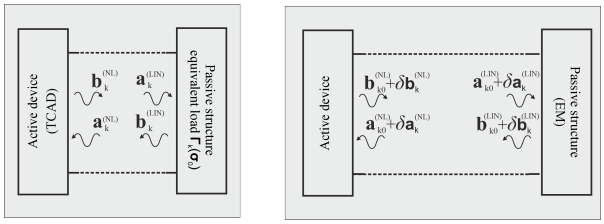

Fig. 1. Schematic representation of the multiphysics MMIC variability modeling approach exploiting TCAD and EM physical analysis. $\mathbf{a}$ and $\mathbf{b}$ are vectors of incident and reflected waves at the interconnecting ports between the active and passive MMIC blocks. $\delta\mathbf{a}$ and $\delta\mathbf{b}$ denote wave variations due to PIV.

II. Multiphysics modelling approach

The multiphysics modeling approach we propose is based on the partition of the MMIC circuit into two interconnected sections, as shown in the left part of Fig. 1 [7]. The left block of the partition contains all the active devices, whereas the right block focuses on the embedding circuit. The two blocks are separately described by physics-based simulations: TCAD for semiconductor devices, and EM for the distributed, or mixed lumped-distributed, passives. The right part of Fig. 1 shows, besides the electrical connection between the two blocks, also an explicit referral to the wave perturbations $\delta\mathbf{a}$ and $\delta\mathbf{b}$ due to technological variations. The nominal device operation is described by the $\mathbf{a}$ and $\mathbf{b}$ waves, calculated with the nominal value of the technological parameters. Wave perturbations are evaluated by the physical simulators as a function of a set of relevant technological parameters; here we select the doping concentration of the active device channel, and the thickness of the SiN layer used for MIM capacitors.

Let us consider first the TCAD description of the active devices. For the sake of simplicity, we focus the attention on the case of a single transistor, however the extension to several active devices is obvious. The physical charge transport model is solved assuming large-signal, in general multi-tone, excitation, and proper loads at the device terminals, thus calling for unconventional TCAD solvers that can hardly be found in commercial device simulators. We consider here the case of a frequency-domain solution of the drift-diffusion transport model making use of the Harmonic Balance technique [8], as this is well suited for the inclusion of PIV due to the availability of efficient numerical techniques for variability analysis [9]–[11]. In order to account for technological variability, TCAD simulations are also parameterized by a proper set of technological parameters, such as the doping level. TCAD

simulations are then used to extract a black-box large-signal model of the active device, in our case the X Parameters [12] (X-Pars), as a function of the technological parameters and for a class AB bias condition selected for the development of a high efficiency PA amplifier (see next Sec. III). X-Pars are then implemented into a circuit design tool, Keysight ADS in our case, by means of a look-up-table approach. An example of validation for this approach is shown in Fig. 2, where the dynamic load lines (DLLs) of the exploited GaAs FET [13] are reported. Notice that the dynamic transcharacteristics make evident the model accuracy in reproducing both the input and output port time-varying variables.

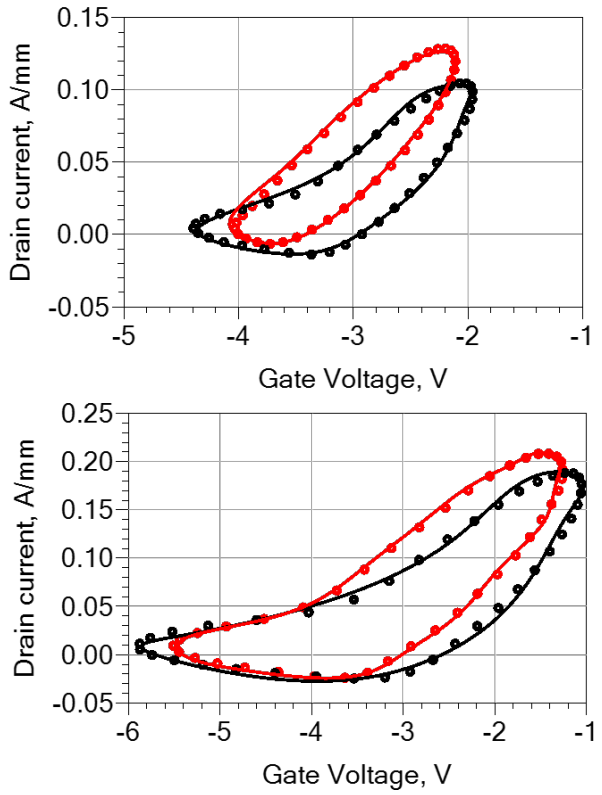

Fig. 2. DLLs in the (I_D, V_{GS}) plane for the active device with varying doping concentration (red: nominal $+5\%$, black: nominal -5%). The device is biased in class AB (10% I_{DSS}). A tuner is used to synthesize the nominal optimum power load at the drain port, while the source is unmatched and terminated with 50 Ω. Top: $P_{av} = 12.5$ dBm; bottom: $P_{av} = 18$ dBm. Lines: X-pars. Symbols: TCAD simulations.

Turning to the case of passive elements, EM simulations of the linear distributed structures are carried out normally in the frequency domain, finally yielding the scattering parameter matrix parameterized by the relevant technological parameters, such as the thickness of the insulator SiN layer used in MIM capacitors. The result of these simulations is a look-up-table model of the frequency- and parameter-dependent two-port scattering matrix, included into ADS via a *citifile* implementing the MDIF standard.

As an example, Fig. 3 shows the Input Matching Network (IMN) designed to synthesize the FET optimum generator impedance, when the FET output port is loaded with the

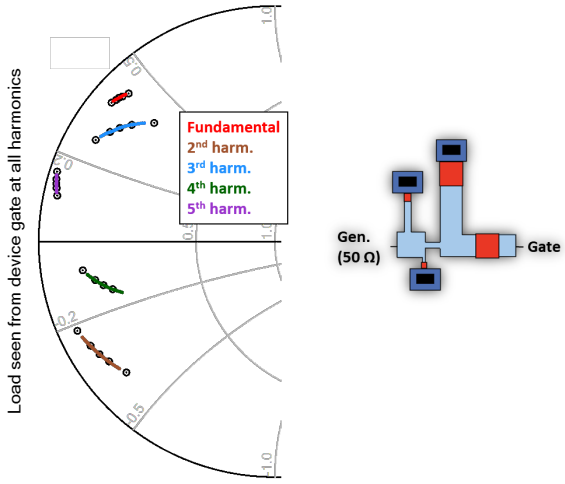

Fig. 3. Variation of the load seen by the device gate at the fundamental frequency 12 GHz and its first 5 harmonics, due to SiN thickness variations in the MIM capacitors. The IMN layout is shown in the inset. Circles refer to the validation test points of 92 nm, 97 nm, 103 nm and 108 nm. Colored dots represent the ADS output of the MonteCarlo analysis.

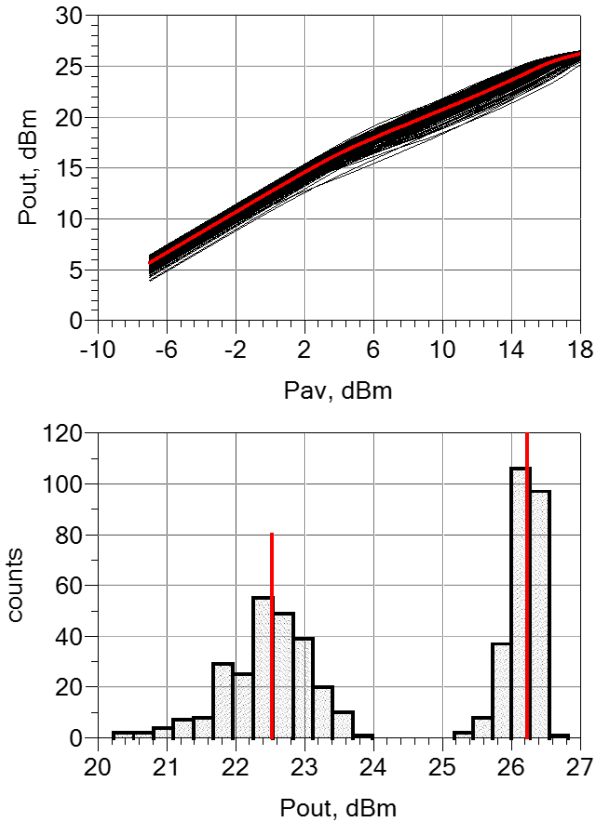

Fig. 4. Top: Distribution of the PA output power. Bottom: P_{out} histograms at 4 dB OBO (left, $P_{av} = 12.5$ dBm) and saturation (right, $P_{av} = 18$ dBm). Red lines denote the nominal values.

optimum power load. The scattering parameters at the fundamental (12 GHz) and up to the fifth harmonic are extracted from EM analysis carried out with ADS Momentum and collected into a look-up table as a function of the MIM thickness. The model is extracted with 7 different thicknesses corresponding to the nominal (100 nm) value ± 2 nm,± 4 nm, ± 6 nm. This spread corresponds to the expected variations provided by the GaAs foundry design kit used in this work. The model is validated against EM simulations for different thickness values, also extending beyond the extraction range, namely 92 nm, 97 nm, 103 nm and 108 nm. The obtained results are shown in Fig. 3. The model allows for fast MonteCarlo analysis within ADS: as an example, Fig. 3 also reports the obtained statistical spread with a MonteCarlo analysis with 1000 gaussian distributed thickness values (2.5 nm variance). Similar accuracy is obtained for the design of the output matching network (OMN).

Once the black-box models are implemented within the design CAD tool, the port wave conservation equations allow for the identification of the self-consistent working point for the entire structure, including of course the effect of parametric variations.

III. Multiphysics PA variability analysis

We have applied the multiphysics modelling approach to the design of a 12 GHz, tuned load, class AB PA implemented in MMIC GaAs technology. The 1 mm active device allows to achieve a nominal output power of 26.5 dBm with 12 dB linear gain and 55% maximum efficiency. In this section we report the outcome of the statistical analysis of the full PA stage (IMN, device, OMN), considering concurrent (uncorrelated) variations of the active device doping and MIM insulator thickness. The MonteCarlo analysis is performed in ADS with 250 independent samples in the 2D parameter space. Both parameters vary according to a gaussian distribution with 2% relative variance.

Figs. 4-6 show the output power, operative gain and drain efficiency distributions as a function of the available input power, along with the corresponding histograms at two selected input powers, namely at 4 dB OBO ($P_{\rm av} = 12.5$ dBm) and at saturation ($P_{\rm av} = 18$ dBm).

The output power distribution is significantly affected by the input drive. In back-off, the distribution is more symmetric and the spread is wider (more than 3 dB). On the other hand, in compression the power distribution is skewed towards lower values, and the spread is also reduced. The residual spread is essentially related to the knee voltage dispersion due to the impact of doping on the channel conductance.

The operative gain shows the typical trend for a deep class AB stage, with soft and hard compression regimes corresponding to the noticeable slope variations. The operative gain spread results from both the output power variations and from the input mismatch. The distribution is rather symmetric for all the observed input powers, and the spread is maximum in back-off and remains almost constant between soft and hard compression, around 1.5 dB.

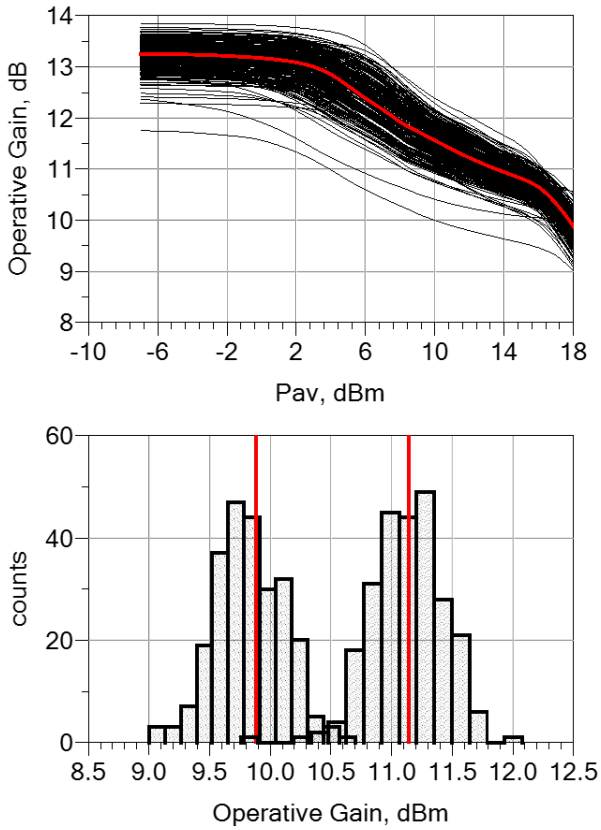

Fig. 5. Top: Distribution of the PA operative gain. Bottom: $G_{\rm op}$ histograms at 4 dB OBO (left, $P_{\rm av} = 12.5$ dBm) and saturation (right, $P_{\rm av} = 18$ dBm). Red lines denote the nominal values.

Finally, the drain efficiency presents an increasing spread with growing input power. The overall variation is extremely significant, since it ranges from 25% to 37% in the 4 dB OBO case, and from 45% to 57% in saturation. To understand the efficiency behavior, we also show the DC power consumption in Fig. 7. Here the spread only slightly depends on the input drive, but it is quite large (around $\pm 20\%$), thus contributing to the overall efficiency variations.

IV. Conclusion

A novel approach to the multiphysics modelling for PIV-aware analysis of MMIC stages has been presented and demonstrated in the design of a 12 GHz, tuned load, class AB PA implemented in MMIC GaAs technology. The models are based on accurate physical simulations and exploit black-box formulations allowing for an efficient implementation in circuit simulators (e.g. Keysight ADS). The model validation has been reported, along with the statistical analysis of the PA stage, which is found to be significantly affected by PIV, already when only two technological parameters (one in the active device, and one in the passive structure) are taken into account. The extension to multiple parameter variations can be readily addressed by our modelling approach, albeit requiring complex multidimensional interpolations over look-up tables.

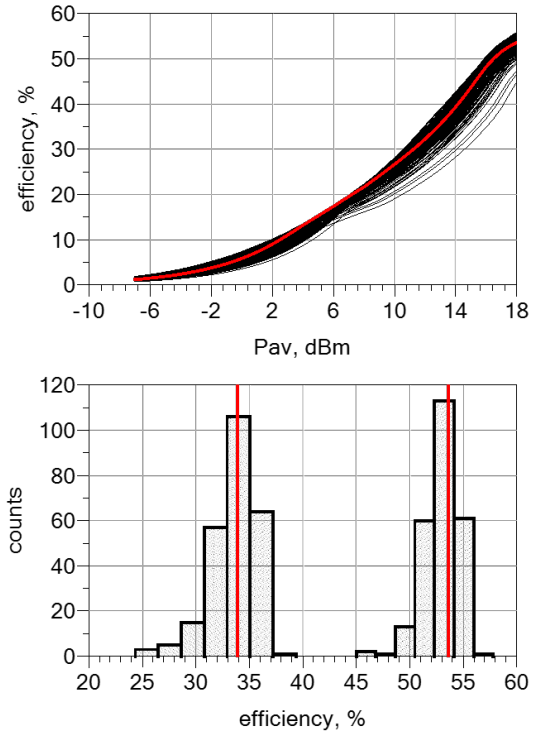

Fig. 6. Top: Distribution of the PA drain efficiency. Bottom: drain efficiency histograms at 4 dB OBO (left, $P_{\mathrm{av}} = 12.5$ dBm) and saturation (right, $P_{\mathrm{av}} = 18$ dBm). Red lines denote the nominal values.

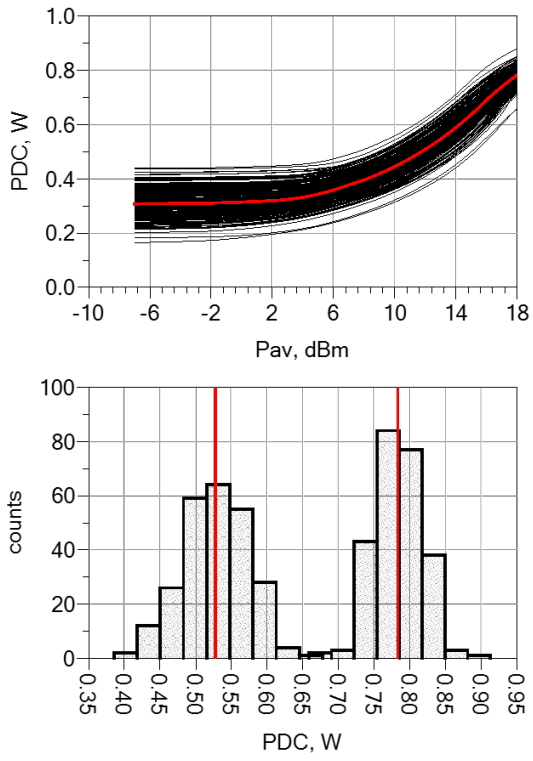

Fig. 7. Top: Distribution of the PA DC power consumption. Bottom: P_{DC} histograms at 4 dB OBO (left, $P_{\mathrm{av}} = 12.5$ dBm) and saturation (right, $P_{\mathrm{av}} = 18$ dBm). Red lines denote the nominal values.

ACKNOWLEDGMENT

This work has been supported by the Italian Ministero dell'Istruzione dell'Università e della Ricerca (MIUR) under the PRIN 2017 Project "Empowering GaN-on-SiC and GaN-on-Si technologies for the next challenging millimeter-wave applications (GANAPP)"

REFERENCES

[1] H.-J. Lee, S. Callender, S. Rami, W. Shin, Q. Yu, and J. M. Marulanda, "Intel 22nm low-power FinFET (22FFL) process technology for 5G and beyond," in *2020 IEEE Custom Integrated Circuits Conference (CICC)*. IEEE, mar 2020.

[2] Z. Wang, H. Wang, and P. Heydari, "CMOS power-amplifier design perspectives for 6G wireless communications," in *2021 IEEE International Midwest Symposium on Circuits and Systems (MWSCAS)*. IEEE, aug 2021.

[3] N. Collaert, A. Alian, A. Banerjee, V. Chauhan, R. Y. ElKashlan, B. Hsu, M. Ingels, A. Khaled, K. V. Kodandarama, B. Kunert, Y. Mols, U. Peralagu, V. Putcha, R. Rodriguez, A. Sibaja-Hernandez, E. Simoen, A. Vais, A. Walke, L. Witters, S. Yadav, H. Yu, M. Zhao, P. Wambacq, B. Parvais, and N. Waldron, "From 5G to 6G: will compound semiconductors make the difference?" in *2020 IEEE 15th International Conference on Solid-State & Integrated Circuit Technology (ICSICT)*. IEEE, nov 2020.

[4] N. Poluri, M. M. DeSouza, N. Venkatesan, and P. Fay, "Modelling challenges for enabling high performance amplifiers in 5G/6G applications," in *2021 28th International Conference on Mixed Design of Integrated Circuits and System*. IEEE, jun 2021.

[5] R. Quaglia, V. Camarchia, T. Jiang, M. Pirola, S. Donati Guerrieri, and B. Loran, "K-band GaAs MMIC doherty power amplifier for microwave radio with optimized driver," *IEEE Transactions on Microwave Theory and Techniques*, vol. 62, no. 11, pp. 2518–2525, nov 2014.

[6] S. Donati Guerrieri, C. Ramella, F. Bonani, and G. Ghione, "Efficient sensitivity and variability analysis of nonlinear microwave stages through concurrent TCAD and EM modeling," *IEEE Journal on Multiscale and Multiphysics Computational Techniques*, vol. 4, pp. 356–363, 2019.

[7] S. Donati Guerrieri, C. Ramella, E. Catoggio, and F. Bonani, "Bridging the gap between physical and circuit analysis for variability-aware microwave design: Modeling approaches," *Electronics*, vol. 11, no. 6, p. 860, mar 2022.

[8] S. Donati Guerrieri, M. Pirola, and F. Bonani, "Concurrent efficient evaluation of small-change parameters and Green's functions for TCAD device noise and variability analysis," *IEEE Transactions on Electron Devices*, vol. 64, no. 3, pp. 1269–1275, mar 2017.

[9] F. Bonani, S. Donati Guerrieri, F. Filicori, G. Ghione, and M. Pirola, "Physics-based large-signal sensitivity analysis of microwave circuits using technological parametric sensitivity from multidimensional semiconductor device models," *IEEE Transactions on Microwave Theory and Techniques*, vol. 45, no. 5, pp. 846–855, may 1997.

[10] S. Donati Guerrieri, F. Bonani, F. Bertazzi, and G. Ghione, "A unified approach to the sensitivity and variability physics-based modeling of semiconductor devices operated in dynamic conditions—Part I: Large-signal sensitivity," *IEEE Transactions on Electron Devices*, vol. 63, no. 3, pp. 1195–1201, mar 2016.

[11] ——, "A unified approach to the sensitivity and variability physics-based modeling of semiconductor devices operated in dynamic conditions.—Part II: Small-signal and conversion matrix sensitivity," *IEEE Transactions on Electron Devices*, vol. 63, no. 3, pp. 1202–1208, mar 2016.

[12] D. Root, J. Verspecht, J. Horn, and M. Marcu, *X-parameters: characterization, modeling, and design of nonlinear RF and microwave components*. Cambridge: Cambridge University Press, 2013.

[13] S. Donati Guerrieri, F. Bonani, and G. Ghione, "Linking X parameters to physical simulations for design-oriented large-signal device variability modeling," in *2019 IEEE MTT-S International Microwave Symposium (IMS)*. IEEE, jun 2019.